Theoretical Study of Mixed $LiLnX_4$ (Ln = La, Dy; X = F, Cl, Br, I) Rare Earth/Alkali Halide Complexes

Cornelis Petrus Groen and Ad Oskam

Institute for Molecular Chemistry, University of Amsterdam, Nieuwe Achtergracht 166, 1018 WV Amsterdam, The Netherlands

Attila Kovács*,†

Research Group for Technical Analytical Chemistry of the Hungarian Academy of Sciences at the Institute of General and Analytical Chemistry of the Budapest Technical University, H-1521 Budapest, Hungary

Received May 31, 2000

The structure, bonding and vibrational properties of the mixed $LiLnX_4$ (Ln = La, Dy; X = F, Cl, Br, I) rare earth/alkali halide complexes were studied using various quantum chemical methods (HF, MP2 and the Becke3-Lee−Yang−Parr exchange-correlation density functional) in conjunction with polarized triple-ζ valence basis sets and quasi-relativistic effective core potentials for the heavy atoms. Our comparative study indicated the superiority of MP2 theory while the HF and B3-LYP methods as well as less sophisticated basis sets failed for the correct energetic relations. In particular, *f* polarization functions on Li and X proved to be important for the Li···X interaction in the complexes. From the three characteristic structures of such complexes, possessing 1- (C_{3v}), 2- (C_{2v}), or 3-fold coordination (C_{3v}) between the alkali metal and the bridging halide atoms, the bi- and tridentate forms are located considerably lower on the potential energy surface then the monodentate isomer. Therefore only the bi- and tridentate isomers have chemical relevance. The monodentate isomer is only a high-lying local minimum in the case of X = F. For X = Cl, Br, and I this structure is found to be a second-order saddle point. The bidentate structure was found to be the global minimum for the systems with X = F, Cl, and Br. However, the relative stability with respect to the tridentate structure is very small (1−5 kJ/mol) for the heavier halide derivatives and the relative order is reversed in the case of the iodides. The energy difference between the three structures and the dissociation energy decrease in the row F to I. The ionic bonding in the complexes was characterized by natural charges and a topological analysis of the electron density distribution according to Bader's theorem. Variation of the geometrical and bonding characteristics between the lanthanum and dysprosium complexes reflects the effect of "lanthanide contraction". The calculated vibrational data indicate that infrared spectroscopy may be an effective tool for experimental investigation and characterization of $LiLnX_4$ molecules.

Introduction

The formation of vapor complexes in quasi-binary systems of metal halides with alkali halides is a well-known phenomenon.[1−4] Best known are the boron and aluminum complexes present in vapors above equimolar mixtures of MX and BX_3 or AlX_3 (M = alkali metal and X = halogen).[5−7] In several high-temperature applications, these halogen-bridged vapor complexes are of fundamental importance.[5,6,8,9] The vapor complexes formed between rare earth halides (LnX_3, Ln = rare earth) and the corresponding alkali halides (MX) are in this respect no exception. Some of their bromide and iodide systems are important components in high-intensity metal halide lamps (see, e.g., ref 10), while the chloride complexes were suggested for high-temperature extraction and separation of rare earths.[11,12]

The industrial importance of the LnX_3−MX systems has resulted in numerous research efforts, all intended to obtain knowledge on the thermodynamic behavior of these systems. The majority of the information known to date originates from Knudsen-effusion mass spectrometry.[4,10,13−17] Other techniques such as gas-phase spectrophotometry and torsion-mass-effu-

† E-mail: attila.aak@chem.bme.hu.

(1) Hargittai, M.; Hargittai, I. *The Molecular Geometries of Coordination Compounds in the Vapour Phase*; Elsevier: Amsterdam, 1977.
(2) Hargittai, M. *Coord. Chem. Rev.* **1988**, *91*, 35.
(3) Hargittai, M. *Chem. Rev.* **2000**, *100*, 2233.
(4) Boghosian, S.; Papatheodorou, G. N. *Halide Vapors and Vapor Complexes*; Elsevier: Amsterdam, 1996; Vol. 23.
(5) Schäfer, H. *Angew. Chem., Int. Ed. Engl.* **1976**, *15*, 713.
(6) Papatheodorou, G. N. Spectroscopy, structure, and bonding of high-temperature metal halide vapor complexes. In *Current Topics in Materials Science*; Kaldis, E., Ed.; North-Holland: Amsterdam, 1982; Vol. 10.
(7) Scholz, G.; Stosser, R. *J. Fluorine Chem.* **1997**, *86*, 131.
(8) Hastie, J. W. *High-Temperature Vapors*; Academic Press: New York, 1975.
(9) Schäfer, H. *Adv. Inorg. Chem.* **1983**, *26*, 201.
(10) Hilpert, K.; Niemann, U. *Thermochim. Acta* **1997**, *299*, 49.
(11) Murase, K.; Machida, K.; Adachi, G. *J. Alloys Compd.* **1995**, *217*, 218.
(12) Murase, K.; Adachi, G.; Hashimoto, M.; Kudo, H. *Bull. Chem. Soc. Jpn.* **1996**, *69*, 353.
(13) Hilpert, K. *J. Electrochem. Soc.* **1989**, *136*, 2099.
(14) Metallinou, M. M.; Herstad, O.; Ostvold, T.; Papatheodorou, G. N. *Acta Chem. Scand.* **1990**, *44*, 683.

10.1021/ic000581t CCC: $19.00
Published on Web 11/30/2000

sion have been applied as well (see ref 4 and references herein).

Information concerning the molecular structure and vibrational characterization of the $MLnX_4$ vapor complexes is still very scarce, although they are important parameters for calculating the thermodynamic functions of these species. This scarcity is not surprising, since experimental methods available for gas-phase structure determination (electron diffraction, microwave spectroscopy) and for vibrational studies (IR and Raman spectroscopy) suffer from technical difficulties at the required high temperatures. Moreover, the complex nature of the vapor composition seriously hampers the interpretation of the results: Besides the $MLnX_4$ species the MX and LnX_3 monomers and M_2X_2 dimer are always present and, with less probability, the Ln_2X_6 dimer, the M_2LnX_5 heterocomplex, and their decomposition products can appear as well.[15]

Only one vibrational spectroscopic investigation is known to date, involving a matrix-isolation infrared study of the systems $MCl-NdCl_3$ (M = Li, Na, Cs) and $LiBr-DyBr_3$.[18] One IR-active stretching mode of the LnX_4 tetrahedron of the $MLnX_4$ vapor species could be identified, but it proved impossible to draw an unambiguous conclusion regarding the molecular symmetry of the observed ternary complexes. A good alternative for a structural and vibrational analysis of the $MLnX_4$ vapor species is offered by theoretical methods. The reliability of computations to obtain molecular data was confirmed by several ab initio and DFT studies of different transition metal and lanthanide compounds.[19−27] Among the halogen-bridged vapor complexes the MBX_4 and $MAlX_4$ compounds have been extensively studied by theoretical methods,[7,28−34] offering a better basis for the interpretation of experimental results.

Theoretical data concerning $MLnX_4$ complexes are, however, limited as well. Our literature search resulted in the sole work of Kapala et al.,[16,35] who performed quantum chemical calculations at the Hartree−Fock level of theory on $NaCeCl_4$ and $NaNdCl_4$. They considered only the bidentate structure neglecting other possible isomers. Additionally, we performed recently a theoretical investigation of $LiCeX_4$ complexes using density functional theory with a less sophisticated basis set as used in this study.[36]

In the present paper we report a systematic computational study of $LiLnX_4$ complexes (Ln = La, Dy; X = F, Cl, Br, I) with the main goal to determine their structural, bonding, and vibrational properties. We compare here the performance of various computational methods (Hartree−Fock and MP2 theory[37] as well as the Becke3-Lee−Yang−Parr exchange-correlation density functional[38,39] in conjunction with quasi-relativistic effective core potentials for the heavy atoms)[40,41] and investigate the influence of basis set size on the various properties of the systems. In the calculations all three possible structures (mono-, bi-, and tridentate) were evaluated. Trends in the halogen group as well as along the lanthanide row are reported for the properties considered. In forthcoming research we plan to investigate the effect of the alkali size on the molecular properties.

Computational Details

The calculations were carried out applying the Hartree−Fock (HF) approximation, the second-order Møller−Plesset perturbation theory in the frozen core approximation (MP2),[37] and the Becke3-Lee−Yang−Parr (B3-LYP)[38,39] density functional using the Gaussian 98 program.[42] For Li the standard 6-311G(d) basis set was used, while for F the 6-311+G(d) basis set was used. Quasi-relativistic effective core potentials (ECP) with a (31111/3111/311) valence basis set were used for the rare earths,[40] while ECPs with (31/311) valence basis were applied for Cl, Br, and I.[41] The ECPs used for the rare earths include the shells 1−4 (that is also the 4f electrons in the case of Dy) in the core, while those of the halogens contain all the electrons below the valence shell. The basis sets were extended with polarization functions. For the initial geometry optimizations and frequency calculations (at HF, MP2, and B3-LYP levels) a single set of *d* polarization functions was added to the halogen atoms.[43] In the following this basis will be denoted as set A.

The final energetic and structural characterization of the complexes was carried out with the valence basis of the rare earths extended with *2fg* while those of the other atoms with *2df* polarization functions (denoted in the following as set B). The two-parameter sets of *f* functions for the rare earth atoms were taken from ref 44, while the *2d* functions for the halides originate from ref 43. The *g* and *f* polarization functions for the rare earth atoms and the halogens, respectively, were optimized according to the procedure described in ref 45 (the

(15) Hilpert, K. Chemistry of Inorganic Vapors. In *Structure and Bonding*; Clarke, M. J., Goodenough, J. B., Ibers, J. A., Jorgensen, C. K., Mingos, D. M. P., Neilands, J. B., Palmer, G. A., Reinen, D., Sadler, P. J., Weiss, R., Williams, R. J. P., Eds.; Springer: Berlin, 1990; Vol. 73; p 97.
(16) Kapala, J.; Roszak, S.; Lisek, I.; Miller, M. *Chem. Phys.* **1998**, *238*, 221.
(17) Lisek, I.; Kapala, J.; Miller, M. *J. Alloys Compd.* **1998**, *280*, 77.
(18) Feltrin, A.; Cesaro, S. N. *High Temp. Mater. Sci.* **1996**, *35*, 203.
(19) Ellis, D. E.; Goodman, G. L. *Int. J. Quantum Chem.* **1984**, *25*, 185.
(20) Russo, T. V.; Martin, R. L.; Hay, P. J. *J. Phys. Chem.* **1995**, *99*, 17085.
(21) Nash, C. S.; Bursten, B. E. *New J. Chem.* **1995**, *19*, 669.
(22) Seth, M.; Dolg, M.; Fulde, P.; Schwerdtfeger, P. *J. Am. Chem. Soc.* **1995**, *117*, 6597.
(23) Lanza, G.; Fragala, I. L. *Chem. Phys. Lett.* **1996**, *255*, 341.
(24) Kovács, A.; Konings, R. J. M.; Booij, A. S. *Chem. Phys. Lett.* **1997**, *268*, 207.
(25) Adamo, C.; Maldivi, P. *Chem. Phys. Lett.* **1997**, *268*, 61.
(26) Adamo, C.; Maldivi, P. *J. Phys. Chem. A* **1998**, *102*, 6812.
(27) Lanza, G.; Fragala, I. L. *J. Phys. Chem. A* **1998**, *102*, 7990.
(28) Ramondo, F.; Bencivenni, L.; Martino, V. D. *Chem. Phys.* **1991**, *158*, 41.
(29) Scholz, G.; Curtiss, L. A. *J. Mol. Struct. (THEOCHEM)* **1992**, *90*, 251.
(30) Spoliti, M.; Sanna, N.; Martino, V. D. *J. Mol. Struct. (THEOCHEM)* **1992**, *90*, 83.
(31) Curtiss, L. A. *Proc. Int. Symp. Molten Salts Chem., Technol.* **1993**, *93-9*, 31.
(32) Bock, C. W.; Trachtman, M.; Mains, G. J. *J. Phys. Chem.* **1994**, *98*, 478.
(33) Charkin, O. P.; McKee, M. L.; Klimenko, M. L.; Schleyer, P. v. R. *Zh. Neorg. Khim.* **1998**, *43*, 1184.
(34) Solomonik, V. G.; Sliznev, V. V. *J. Struct. Chem.* **1999**, *40*, 368.
(35) Kapala, J.; Lisek, I.; Roszak, S.; Miller, M. *Polyhedron* **1999**, *18*, 2845.
(36) Groen, P.; Oskam, A.; Kovács, A. *J. Mol. Struct. (THEOCHEM)* **2000**, *531*, 23.
(37) Møller, C.; Plesset, M. S. *Phys. Rev.* **1934**, *46*, 618.
(38) Becke, A. D. *J. Chem. Phys.* **1993**, *98*, 5648.
(39) Lee, C.; Yang, W.; Parr, R. G. *Phys. Rev. B* **1998**, *37*, 785.
(40) Dolg, M.; Stoll, H.; Savin, A.; Preuss, H. *Theor. Chim. Acta* **1989**, *75*, 173.
(41) Bergner, A.; Dolg, M.; Küchle, W.; Stoll, H.; Preuss, H. *Mol. Phys.* **1993**, *80*, 1431.
(42) Frisch, M. J.; Trucks, G. W.; Schlegel, H. B.; Scuseria, G. E.; Robb, M. A.; Cheeseman, J. R.; Zakrzewski, V. G.; Jr, J. A. M.; Stratmann, R. E.; Burant, J. C.; Dapprich, S.; Millam, J. M.; Daniels, A. D.; Kudin, K. N.; Strain, M. C.; Farkas, O.; Tomasi, J.; Barone, V.; Cossi, M.; Cammi, R.; Mennucci, B.; Pomelli, C.; Adamo, C.; Clifford, S.; Ochterski, J.; Petersson, G. A.; Ayala, P. Y.; Cui, Q.; Morokuma, K.; Rabuck, A. D.; Raghavachari, K.; Foresman, J. B.; Cioslowski, J.; Ortiz, J. V.; Stefanov, B. B.; Liu, G.; Liashenko, A.; Piskorz, P.; Komaromi, I.; Gomperts, R.; Martin, R. L.; Fox, D. J.; Keith, T.; Al-Laham, M. A.; Peng, C. Y.; Nanayakkara, A.; Gonzalez, C.; Challacombe, M.; Gill, P. M. W.; Johnson, B.; Chen, W.; Wong, M. W.; Andres, J. L.; Gonzalez, C.; Head-Gordon, M.; Replogle, E. S.; Pople, J. A. *Gaussian 98*, revision A.5; Gaussian Inc.: Pittsburgh, PA, 1998.
(43) Andzelm, J.; Huzinaga, S.; Klobukowski, M.; Radzio, E.; Sakai, Y.; Tatekawi, H. *Gaussian Basis Sets for Molecular Calculations*; Elsevier: Amsterdam, 1984.
(44) Dolg, M. Ph.D. Dissertation, University of Stuttgart, 1989.
(45) Ehlers, A. W.; Böhme, M.; Dapprich, S.; Gobbi, A.; Höllwarth, A.; Jonas, V.; Köhler, K. F.; Stegmann, R.; Veldkamp, A.; Frenking, G. *Chem. Phys. Lett.* **1993**, *208*, 111.

exponents: $\alpha_{La} = 0.731$, $\alpha_{Dy} = 1.043$, $\alpha_{Cl} = 0.720$, $\alpha_{Br} = 0.581$, $\alpha_I = 0.426$). In all the calculations the default pure 5 *d* and 7 *f* functions were used. We note that studies on metal halide systems (except the very small two or three atomic systems) have been performed with less sophisticated basis sets until now (usually with only a single set of *f* functions on the metal and *d* functions on the halogen).[3] Test calculations with a gradually increasing basis set and the BSSE data (vide infra) showed, however, that even set B is not sufficiently saturated.

Important differences were found in the energetic relations of the various possible structures as a function of the basis set and method (vide infra). Test calculations on $LiDyI_4$ were carried out extending gradually set A toward set B. It was indicated that *f* polarization functions on both Li and I are important to predict the correct trend between the possible structures. The reliability of HF, MP2, and B3-LYP theories for predicting the energetics of the various structures was checked by test calculations on the $LiDyX_4$ complexes using CCSD-(T) theory.[46] Because of economical considerations the basis set used contained a single set of *f* functions for Dy and 2*df* polarization functions for Li and I. Single-point calculations using the MP2 optimized geometries of structures 2 and 3 confirmed the reliability of the MP2/B results. Because of the observed limitations of the HF and B3-LYP methods, calculations on the lanthanum complexes as well as the bonding and vibrational analyses were only performed at the MP2 level.

The basis set superposition error was calculated according to the counterpoise method.[47] The natural bond orbital (NBO) analysis[48] was performed with the routine built in Gaussian 94,[49] while for the topological analysis of the electron density distribution[50] we used the AIMPAC program package.[51] Due to some technical problems of the NBO program to handle the present ECPs for f-shell elements and the inability of both the NBO and AIMPAC programs to handle *g* functions, the NBO and topological analyses were exclusively carried out for the $LiLaX_4$ complexes. The wave functions for the analyses were obtained by MP2 single-point calculations using a reduced basis (neglecting the *g* polarization functions from set B, denoted in the following as B′) on the MP2/B geometries. Test calculations revealed that the effect of the reference geometry, MP2/B versus MP2/B′, is negligible for the above properties.

Results and Discussion

1. Structures and Energetics. The three characteristic structures of the $LiLnX_4$ complexes are presented in Figure 1. In the individual isomers one (structure 1), two- (structure 2), or three (structure 3) halogen atoms can act as a bridge between the alkali atom and the rare earth atom. Structures 1 and 3 have C_{3v} while structure 2 possesses a C_{2v} symmetry. In our previous study of the $LiCeX_4$ complexes we have investigated the potential energy surface (PES) searching for other possible (nonsymmetrical) local minima beyond the three stationary points.[36] These previous calculations confirmed the exclusive possibility of structures 2 and 3 (and 1 if X = F) for the $LiCeX_4$ complexes.

The present calculations agree with previous results[36] in the minimum character of structures 2 and 3 of $LiLnX_4$ compounds.

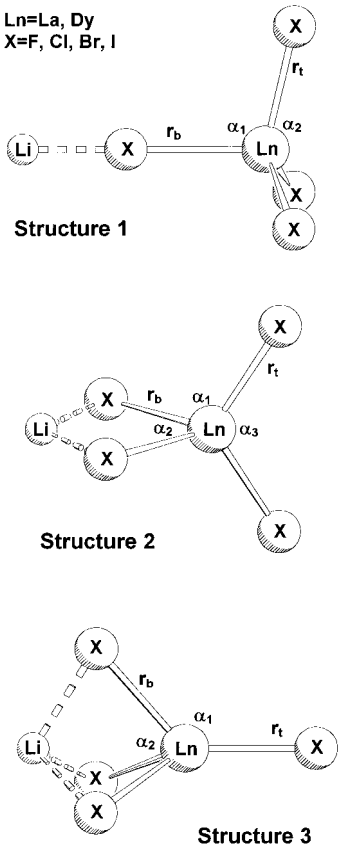

Figure 1. Characteristic structures and labeling of the geometrical parameters of the $LiLnX_4$ (Ln = La, Dy; X = F, Cl, Br, I) coordination complexes.

Similarly, structure 1 was found to be a second-order saddle point for the complexes X = Cl, Br, and I while in the case of the $LiLnF_4$ complexes, unlike the experience on analogous $MAlF_4$ derivatives,[34] it proved to be a high-lying local minimum. The different character of the fluoride derivatives can be understood upon the very large electronegativity of F compared to the other halogens. Obviously, the much stronger bonding interaction between the fluorine and lithium is responsible for a change in character of the PES around this stationary point.

The computed relative energies of structures 1, 2, and 3 of the $LiDyX_4$ and $LiLaX_4$ complexes are compiled in Table 1. The trends predicted by the HF/B and B3-LYP/B methods are in agreement with the trends obtained by the present lower level calculations (HF/A, MP2/A, B3-LYP/A) and with those obtained recently for $LiCeX_4$ complexes.[36] At these levels of theory structure 2 is favored energetically irrespective of the halide.

At the MP2/B level the calculations resulted in somewhat different trends. A more decreased stability of structure 1 of the heavier halides with respect to structures 2 and 3 and a considerably larger gain in stability of structure 3 with respect to structure 2 were found. As a result, the relative energies of structures 2 and 3 of the chloride, bromide, and iodide complexes drop to within 5 kJ/mol, and the relative order of stability is reversed in the case of the iodide complexes (cf. Table 1). The relative stabilization of the tridentate isomer with increasing halogen size was also found in a recent MP2 study of the analogous $MAlX_4$ complexes.[32]

The significant differences between the MP2 and B3-LYP results are contrary to the general experience upon comparing both methods. The MP2 and DFT calculated properties (energetics, molecular geometry, and vibrational spectra) are known to be generally in good agreement.[3,52] We are not aware of any

(46) Pople, J. A.; Head-Gordon, M.; Raghavachari, K. *J. Chem. Phys.* **1987**, *87*, 5968.
(47) Boys, S. F.; Bernardi, F. *Mol. Phys.* **1970**, *19*, 553.
(48) Reed, A. E.; Curtiss, L. A.; Weinhold, F. *Chem. Rev.* **1988**, *88*, 899.
(49) Frisch, M. J.; W. Trucks, G.; Schlegel, H. B.; Gill, P. M. W.; Johnson, B. G.; Robb, M. A.; Cheeseman, J. R.; Keith, T.; Petersson, G. A.; Montgomery, J. A.; Raghavachari, K.; Al-Laham, M. A.; Zakrzewski, V. G.; Ortiz, J. V.; Foresman, J. B.; Cioslowski, J.; Stefanov, B. B.; Nanayakkara, A.; Challacombe, M.; Peng, C. Y.; Ayala, P. Y.; Chen, W.; Wong, M. W.; Andres, J. L.; Replogle, E. S.; Gomperts, R.; Martin, R. L.; Fox, D. J.; Binkley, J. S.; Defrees, D. J.; Baker, J.; Stewart, J. P.; Head-Gordon, M.; Gonzalez, C.; Pople, J. A. *Gaussian 94*, revision B.2; Gaussian, Inc.: Pittsburgh, PA, 1995.
(50) Bader, R. F. W. *Atoms in Molecules: A Quantum Theory*; Oxford University Press: Oxford, 1990.
(51) Biegler-König, F. W.; Bader, R. F. W.; Ting-Hua, T. *J. Comput. Chem.* **1982**, *3*, 317.

Table 1. Calculated Relative Energies (kJ/mol) of the $LiDyX_4$ and $LiLaX_4$ Complexes[a]

		structure		
complex	method	1	2	3
$LiDyF_4$	HF	85.2	0.0	37.4
	MP2	87.7	0.0	29.8
	B3-LYP	83.8	0.0	35.6
$LiDyCl_4$	HF	88.4	0.0	21.3
	MP2	100.4	0.0	3.3
	B3-LYP	80.8	0.0	18.2
$LiDyBr_4$	HF	94.1	0.0	16.9
	MP2	103.5	0.0	1.4
	B3-LYP	98.0	0.0	13.5
$LiDyI_4$	HF	95.6	0.0	12.6
	MP2	113.1	4.2	0.0
	CCSD(T)[b]		4.9	0.0
	B3-LYP	100.4	0.0	8.9
$LiLaF_4$	MP2	94.2	0.0	35.1
$LiLaCl_4$	MP2	101.3	0.0	4.6
$LiLaBr_4$	MP2	102.8	0.0	3.8
$LiLaI_4$	MP2	110.6	3.8	0.0

[a] With respect to most stable structure. The absolute energies were calculated using basis set B (except CCSD(T), vide infra) and were corrected for zero-point vibrational energy obtained from calculations using basis set A. [b] Single-point calculations on MP2 optimized geometry. For details of basis set see text.

paper reporting such an unexpected turn of the relative energies of structural isomers. We should note, however, that in general smaller basis sets (up to a single set of *f* polarization functions on the metal and *d* polarization functions on main group elements) have been applied in past calculations due to hardware and algorithm limitations. Our CCSD(T) test calculations resulted in a preference of structure 3 over structure 2 by 4.9 kJ/mol, thereby confirming the MP2 results.

On the basis of its found superiority, the molecular geometries of the lanthanum complexes and the dissociation energies were only calculated at the MP2/B level. The relative energies of the $LiLaX_4$ complexes reflect the same trends as observed for the $LiDyX_4$ complexes. Even though structures 2 of the lanthanum complexes are slightly more stable with respect to structures 1 and 3 than those of the dysprosium compounds, structure 3 remains the absolute minimum for the iodide complex $LiLaI_4$ by 3.8 kJ/mol.

Before a discussion of other molecular properties we comment on the calculated relative stabilities from an experimental point of view. First of all, it should be taken into account that the calculated results refer to the isolated molecule at zero K. The energy differences of structures 2 and 3 are relatively small, and at the temperature of gas-phase experiments (ca. 800−1500 K) an equilibrium between both structures can be expected. To illustrate this, the equilibrium constants of the isomerization reactions of the $LiDyX_4$ species were evaluated over a wide temperature range using thermodynamic functions which were calculated by employing the usual statistical mechanical formulas (rigid rotator, harmonic oscillator approximation) (e.g., ref 53). The molecular constants needed for this calculation were taken from the MP2/B calculations, and the vibrational frequencies (vide infra) were used from the MP2/A calculations. The vibrational frequencies were left unscaled, since recent computational studies on rare earth trihalides[23−27,54] have shown that computations of a quality similar to the MP2/A calculations reproduce the experimental vibrational data of such compounds quite well.

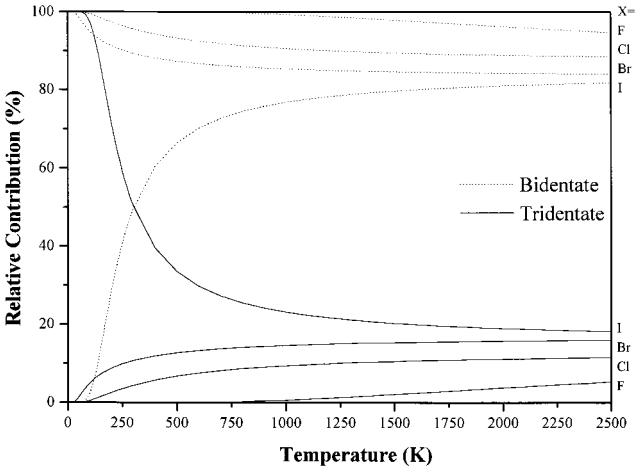

Figure 2. Temperature dependence of the relative content of structures 2 and 3 of $LiDyX_4$ (X = F, Cl, Br, I) molecules under equilibrium conditions.

Table 2. Calculated Dissociation Energies (kJ/mol) of the $LiDyX_4$ and $LiLaX_4$ Complexes[a]

	structure		
complex	1	2	3
$LiDyF_4$	189.7	265.5	227.8
$LiDyCl_4$	136.2	218.7	199.9
$LiDyBr_4$	118.0	209.7	199.2
$LiDyI_4$	101.0	196.6	190.3
$LiLaF_4$	162.9	245.1	201.6
$LiLaCl_4$	126.2	209.7	189.7
$LiLaBr_4$	112.8	203.5	191.4
$LiLaI_4$	99.0	192.7	186.4

[a] Computed at the MP2/B level and corrected for BSSE (MP2/B) and zero-point vibrational energy (MP2/A).

The relative contributions of structures 2 and structures 3 as a function of the temperature are depicted in Figure 2. From this figure it can be concluded that in the temperature range where, based on mass-spectrometric results, a substantial vapor pressure of the complexes is expected (>800 K) (e.g., ref 4), structure 2 is the most abundant vapor complex for all the halides. At 1000 K, the relative amount of structure 3 is ca. 1%, 9%, 15%, and 23% respectively for the fluoride, chloride, bromide, and iodide complex. Responsible for the predicted high relative content of structures 2 is the entropy. As a result of the change in symmetry upon going from structure 2 to structure 3, the entropy change of the isomerization process structure 2 ↔ structure 3 is negative, meaning that it favors the equilibrium in the direction of structure 2. In the case of the fluoride, chloride, and bromide complexes the enthalpy change of the reaction also shifts the equilibrium in the direction of structure 2, but as already indicated by the energy differences at zero K, for the iodide complex the opposite holds. At high temperatures, however, the contribution of $T\Delta S°(T)$ to $-RT \ln K_p = \Delta H°(T) - T\Delta S°(T)$ dominates over the enthalpy change of the reaction $\Delta H°(T)$, leading to a predicted high amount of structure 2 in the case of $LiDyI_4$ as well.

The dissociation energies of the $LiLnX_4$ species to the simple halides LiX and LnX_3 are compiled in Table 2. They give additional information on the stability of the title complexes. Note that these data are corrected for basis set superposition error (BSSE) calculated at the MP2/B level. The BSSE values varied between 11 and 54 kJ/mol, thus playing a non-negligible

(52) Frenking, G.; Fröhlich, N. *Chem. Rev.* **2000**, *100*, 714.
(53) Knox, J. H. *Molecular Thermodynamics*, 2nd ed.; John Wiley & Sons: New York, 1978.
(54) Kovács, A. *Chem. Phys. Lett.* **2000**, *319*, 238.

Table 3. Calculated Geometrical Parameters[a] of the $LiDyX_4$ and $LiLaX_4$ Complexes and the Respective Simple Halides

	$LiDyX_4$				$LiLaX_4$			
	F	Cl	Br	I	F	Cl	Br	I
				Structure 1				
r_t	2.053	2.476	2.628	2.845	2.173	2.614	2.767	2.983
r_b	2.234	2.650	2.817	3.040	2.414	2.818	2.988	3.204
Li−X	1.654	2.084	2.252	2.467	1.649	2.079	2.255	2.470
α_1	102.8	102.8	103.0	103.1	103.2	102.8	103.3	103.1
α_2	115.2	115.3	115.1	115.0	115.0	115.3	114.9	115.0
Ln−X−Li	180.0	180.0	180.0	180.0	180.0	180.0	180.0	180.0
				Structure 2				
r_t	2.033	2.460	2.611	2.829	2.148	2.594	2.748	2.965
r_b	2.180	2.602	2.767	2.983	2.333	2.759	2.922	3.138
Li−X	1.774	2.204	2.390	2.609	1.764	2.201	2.385	2.604
α_1	114.5	112.5	111.9	111.0	115.4	113.5	113.0	112.0
α_2	74.6	84.8	89.0	93.5	70.4	80.7	84.4	88.9
α_3	117.2	117.5	116.9	117.0	116.7	116.8	116.5	116.6
X−Li−X	96.3	105.6	108.5	112.9	99.4	108.4	110.9	115.2
Ln−X−Li	94.5	84.8	81.3	76.8	95.1	85.5	82.4	78.0
				Structure 3				
r_t	2.058	2.476	2.627	2.841	2.178	2.617	2.771	2.986
r_b	2.116	2.543	2.705	2.924	2.254	2.687	2.849	3.066
Li−X	1.953	2.396	2.597	2.815	1.939	2.384	2.585	2.806
α_1	132.4	127.9	126.0	124.0	135.2	130.9	128.8	126.8
α_2	79.5	86.3	89.0	91.7	75.2	81.9	84.9	87.8
X−Li−X	87.7	93.0	93.8	96.4	90.4	95.2	96.1	98.5
Ln−X−Li	79.3	71.0	68.5	64.6	80.2	72.3	69.6	65.8
				LnX_4^-				
Ln−X	2.091	2.515	2.669	2.889	2.221	2.658	2.813	3.030
				LiX				
Li−X	1.590	2.020	2.193	2.414				

[a] Calculated at the MP2/B level. Bond lengths are given in angstroms, bond angles in degrees. For the abbreviation of geometrical parameters see Figure 1.

contribution to the uncorrected dissociation energy. Generally, the BSSE values were around 12, 25, and 35 kJ/mol for the mono-, bi-, and tridentate forms, respectively, except the chloride complexes, where approximately 50% higher values were found.

The high dissociation energies (between 99 and 266 kJ/mol, cf. Table 2) indicate strong interactions in the complexes and a large stability against decomposition, although this may not be reflected in high-temperature experiments. In agreement with the expectations based on the electrostatic character of the bonding, the strongest bonding interactions are present in the fluoride complexes, while there is a considerable drop upon going from the fluorides to chlorides. The decrease becomes gentle from the chlorides to the iodides. The trend in the lanthanide row appears in consistently higher dissociation energies of the $LiDyX_4$ compounds compared to those of the $LiLaX_4$ derivatives.

2. Geometry. The calculated geometrical parameters of the $LiLnX_4$ complexes as well as those of the simple reference halides (the tetrahedral LnX_4^- anions and LiX) are compiled in Table 3. Our discussion includes also the geometrical parameters of structures 1. Although the practical importance of these isomers is negligible due to their high energy and mostly saddle-point character, they are the forms where the single Li···X interaction can be studied without the geometrical constraints present in the other two isomers.

In view of the found deficiencies of smaller basis sets as well as the HF and B3-LYP methods, our discussion is focused on the molecular geometries obtained at the MP2/B level. We note only some characteristics of the less superior levels. The smaller basis set A resulted generally in longer Ln−X bonds compared with those obtained using set B (ca. 0.01 Å with HF and B3-LYP, and ca. 0.05 Å with MP2) while only minor variations were found in the Li−X distances and in the bond angles. With respect to MP2/B, considerably longer Ln−X bonds were obtained at the HF/B and B3-LYP/B levels, varying from ca. 0.01 Å in the fluorides up to 0.14 Å in the other halides (the B3-LYP values being somewhat closer to the MP2 ones). The calculated HF/B and B3-LYP/B Li−X distances are generally shorter in the fluorides (up to 0.03 Å) but longer in the other halides (up to 0.07 Å). On the other hand, only minor differences (generally within 1°) appear in the bond angles.

The most important bonding interaction in title coordination complexes is the principally electrostatic interaction between the lithium cation and the LnX_4^- anions. Characteristics of this interaction in the individual structures (1 to 3) are reflected by the Li−X distances as well as by changes in the geometrical parameters of the LnX_4^- moieties in the complexes with respect to the parent free LnX_4^- ions.

The most obvious consequence of the Li···X interaction is the lengthening of the Ln−X bonds of the bridging halogens (r_b) with respect to the Ln−X bonds in the free LnX_4^- ions (cf. Table 3). Additional geometrical consequences are the shortening of the terminal Ln−X bonds (r_t) and deformation of the originally tetrahedral LnX_4^- geometry. Similarly to the weakened Ln−X bonds in the Ln−X−Li units, the Li−X distances are also longer in the complexes (especially in the bi- and tridentate structures) than in the respective lithium halide.

The change of the various geometrical parameters in the structure 1−3 series of a given $LiLnX_4$ complex is determined primarily by the fact that the Li···X interaction weakens with increasing coordination number of Li. Thus the Li−X distances are the shortest in structures 1 and the longest in structures 3. Accordingly, r_b changes in the opposite direction: it is larger by ca. 7%, 4%, and 1% in structures 1, 2, and 3, respectively, compared to the Ln−X bonds of the parent LnX_4^- anion. The shortening of the terminal Ln−X bonds (r_t) (ca. 2% with respect to LnX_4^-) is essentially independent of the type of Li coordination. In accordance with the observed lengthening of r_b, the bond angles between a terminal and a bridging halogen (α_1) are smaller in structures 1 compared to the tetrahedral value (109.47°) of the free LnX_4^-. In structures 2 and 3 the bridging halogens are geometrically constrained to lithium, resulting in a larger than tetrahedral value for α_1.

The magnitude of steric effects strongly correlates with the previously determined energetic relations of the various structures. As was shown before, structures 2 and 3 gain stability with respect to structure 1 in the case of heavier halogens (cf. Table 1). The larger possible bond interactions of the heavier halogens, leading to a decrease in steric strain of structures 2 and 3, are responsible for this. As a measure, the ratios of the Li−X distances of structures 2 and 3 can be compared to the Li−X distances of structures 1, where steric effects play a negligible role. For example, the Li−X bond in structure 2 of $LiDyF_4$ is found to be longer by 7.2% than in structure 1, while this ratio is reduced to 5.8% in the case of $LiDyI_4$. The α_1 and α_2 bond angles indicate a decreasing strain as well (tend to approach the tetrahedral value) in structures 2 and 3 toward the heavier halides.

For the main differences in the geometrical parameters of the respective $LiLaX_4$ and $LiDyX_4$ complexes the "lanthanide contraction" is responsible. Thus, the r_t and r_b bond distances of the La complexes are longer by 0.12−0.18 Å than those of the Dy complexes. On the other hand, only minor differences can be observed in the Li−X distances with different rare earths. The affected bond angles change accordingly: hence the α_2 angles of structures 2 and 3 are smaller by ca. 4°, the X−Li−X

Table 4. NBO Atomic Charges of the $LiLaX_4$ Complexes and the Respective Simple Halides[a]

	$LiLaX_4$			
	F	Cl	Br	I
		Structure 1		
q(Li)	0.982	0.965	0.957	0.938
q(La)	2.625	2.387	2.303	2.118
q(X_b)	−0.951	−0.899	−0.887	−0.848
q(X_t)	−0.885	−0.818	−0.791	−0.736
		Structure 2		
q(Li)	0.957	0.897	0.876	0.822
q(La)	2.631	2.378	2.292	2.095
q(X_b)	−0.920	−0.835	−0.809	−0.742
q(X_t)	−0.874	−0.803	−0.775	−0.717
		Structure 3		
q(Li)	0.939	0.862	0.841	0.778
q(La)	2.637	2.384	2.303	2.109
q(X_b)	−0.897	−0.807	−0.782	−0.715
q(X_t)	−0.885	−0.825	−0.799	−0.743
		LiX		
q(Li)	0.976	0.948	0.931	0.899
q(X)	−0.976	−0.948	−0.931	−0.899
		LaX_4^-		
q(La)	2.615	2.376	2.288	2.100
q(X)	−0.904	−0.844	−0.822	−0.775

[a] Calculated at the MP2/B′ level; for details of basis set see text. The abbreviations b and t mean bridged and terminal, respectively (cf. Figure 1).

angles larger by ca. 3° in the $LiLaX_4$ derivatives. The other bond angles agree within 1° in the respective $LiLaX_4$ and $LiDyX_4$ complexes.

The fairly constant Li−X distances indicate a minor influence of the lanthanide type on the Li···X interaction. In most of the cases the Li−X distances are slightly longer in the Dy complexes, indicating a somewhat weaker interaction, while, according to the calculated dissociation energies, the Dy complexes should be more stable than the La derivatives (cf. Table 2). These facts point to the importance of the Ln···X interaction and prove that the dissociation energies into the LiX and LnX_3 components are determined by the strengths of the Ln−X bonds.

3. Bonding Analysis. Information on the bonding in the title molecules can be obtained from the analysis of the electron density distribution. We investigated the ionic interactions in the $LiLaX_4$ complexes using NBO atomic charges which are considered to be sufficiently reliable and stable to computational parameters.[48] Unfortunately, the NBO subunit of the Gaussian94 and 98 programs failed to calculate the natural charges for the dysprosium complexes using the present ECP of the rare earth with f electrons included in the core.[40] The other choice, an analysis based on Mulliken atomic charges, was omitted here because of known limitations of the Mulliken population analysis,[55] especially concerning metal−ligand interactions.[56] We note here that recent studies on rare earth trihalides report a decreasing ionic character toward the higher rare earths.[25,26]

The present NBO charges demonstrate a decreasing ionic character of the metal−halogen bonds going from F to I (cf. Table 4). Within a structure 1−3 series the data show a significant variation of the atomic charges in the different structures. The largest effect can be seen on Li and the bridging halogens: their charge is gradually decreasing in absolute value with the coordination number of Li. This points unambiguously to a decreasing electrostatic character of the Li···X interaction from structure 1 to 3. On the other hand, the charges of La and the terminal halogens show much smaller variation, supporting the conclusion (indicated already by the bond distances, vide supra) that this moiety of the complexes is only marginally influenced by the Li···X interaction. These bonds have slightly smaller ionic character in structures 2 than in the other two forms.

Comparison with the LiX and LaX_4^- reference molecules reveals an increase in the ionic character of the Li−X and La−X_b bonds in structures 1. The opposite holds for the Li−X and La−X_b bonds in structures 2, which show a slight decrease in ionic character. A larger decrease is found for the Li−X and La−X_b bonds in structures 3 and for all the terminal La−X bonds. In agreement with the above trend, the ring halogens are more negatively charged than the terminal ones in structures 1 and 2, while this relative order is reversed for structures 3. The largest differences in the ionic/covalent character of the ring and terminal La−X bonds appear in the case of structures 1.

Other characteristics of the electron density distribution can be seen in Figure 3 where the contour line diagrams of the Laplacian distribution for the three structures of $LiLaCl_4$ are depicted. Most obvious is the contraction of the charge toward the nuclei and the somewhat deformed charge distribution around lanthanum according to the negatively charged chloride ions.

Results of the topological analysis of the electron density distribution are compiled in Table 5. We note the deficiency of the searching algorithm for locating several bond critical points. Its reason may be the low electron density around the critical points, as is usual with closed-shell interactions.

Characteristics of the bond critical points are in agreement with strong electrostatic interactions between La and the halogens. Thus the charge densities ρ are relatively low in value, and the Laplacian $\nabla^2\rho$ values are positive.[50] Variation of these parameters in the $LiLaX_4$ series (X = F to I) corresponds to the increasing metal−halogen bond distances with larger halogens. The small variation in the ionic/covalent character of the bonding cannot be distinguished in the ρ and $\nabla^2\rho$ properties of the bond critical points. On the other hand, the slight distortion of the electron density distribution from C_∞ symmetry in the La−X_b and Li−X bonds of structures 2 and 3 (cf. the ellipticity values in Table 4) is in agreement with minor covalent contributions in the bonding.

4. Vibrational Spectra. In this section we investigate the possibilities of vibrational spectroscopy for the identification and characterization of the title coordination complexes. We discuss only the vibrational spectra of the most relevant structures 2 and 3. For visual presentation (Figure 4) the IR and Raman spectra of $LiLaF_4$ and $LiLaI_4$ were selected. The spectra of the bromides and chlorides are similar to the presented ones of $LiLaI_4$. Differences between the spectral features of $LiLnF_4$ and the other three halide complexes can be attributed to the different mixing of internal coordinates in the normal modes of the various complexes with light (F) or heavy (Cl, Br, I) halogens. Additionally, the large polarity of the metal−fluorine bonds results in an increased sensitivity of IR spectroscopy for fluoride complexes, while the opposite holds for the Raman technique. The change of the rare earth from La to Dy results in a small increase of the frequency values and in

(55) Mulliken, R. S. *J. Chem. Phys.* **1955**, *23*, 1833.

(56) A recent theoretical study of Adamo and Maldivi showed the inadequacy of Mulliken atomic charges for rare earth halides predicting trends incorrectly upon variation both the rare earth and the halogen.[25] In the case of the present complexes, the fluorines of structures 1 and 3 were found to be less negatively charged than the respective chlorines in full contrast with usual chemical experience.

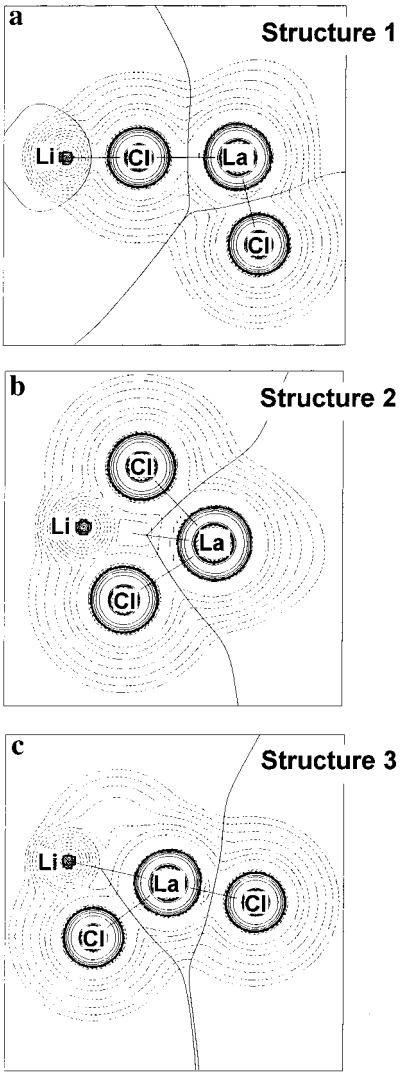

Figure 3. Contour line diagrams of the Laplacian distribution $\nabla^2\rho(r)$ for the three characteristic structures of $LiLaCl_4$: (a) structure 1 in the Li−Cl−La−Cl plane; (b) structure 2 in the Li−(Cl_2)−La plane; (c) structure 3 in the Li−Cl−La−Cl plane. Dashed lines indicate charge depletion ($\nabla^2\rho(r) > 0$); solid lines indicate charge concentration ($\nabla^2\rho(r) < 0$). The solid lines connecting the atomic nuclei are bond paths (where the bond critical points were found). The solid lines separating the atoms show the zero-flux surfaces in the plane.

minor differences in the relative intensities. The calculated vibrational frequencies as well as IR and Raman activities of all the molecules are available in the Supporting Information.

First we should note the difficulties in the interpretation of the vibrational spectra of $MLnX_4$ compounds due to the complex composition of their vapor. According to mass spectroscopic studies on related complexes[15] the LnX_3, MX, and M_2X_2 species might be present in considerable amounts in equilibrium vapors over $MX-LnX_3$ systems. Their vibrational bands appear in the same, and rather small (ca. 500 cm^{-1}), spectral region as those of the respective $MLnX_4$ molecules with possible overlaps of close-lying fundamentals.[36] Moreover, as pointed out earlier, both isomers of the $MLnX_4$ species are expected to be present in the vapor, especially in the case of the bromides and iodides. All these features point to the importance of a selection of the experimental method: preferably a technique providing narrow signals (matrix-isolation or supersonic jet) over "simple" gas-phase experiments. Additionally, a careful preinvestigation of the LnX_3 and MX halides (under similar experimental conditions for locating the exact position of their bands) is required in order to distinguish the $MLnX_4$ bands unambiguously.

Table 5. Results from the Topological Analysis of the Electron Density in the $LiLaX_4$ Complexes[a]

	$LiLaX_4$			
	F	Cl	Br	I
		Structure 1		
r_b				
$\rho(r_c)$	0.316	0.192	0.162	0.139
$\nabla^2\rho(r_c)$	5.406	2.578	1.938	1.437
ϵ	0.000	0.000	0.000	0.000
r_t				
$\rho(r_c)$	0.517	0.331	0.296	0.258
$\nabla^2\rho(r_c)$	8.640	4.165	3.044	2.090
ϵ	0.025	0.026	0.021	0.016
Li−X				
$\rho(r_c)$	0.361	0.200	0.169	0.147
$\nabla^2\rho(r_c)$	12.139	4.826	3.572	2.492
ϵ	0.000	0.000	0.000	0.000
		Structure 2		
r_b				
$\rho(r_c)$		0.236	0.211	
$\nabla^2\rho(r_c)$		2.980	2.275	
ϵ		0.062	0.063	
r_t				
$\rho(r_c)$		0.347	0.309	0.268
$\nabla^2\rho(r_c)$		4.340	3.144	2.143
ϵ		0.020	0.014	0.008
		Structure 3		
r_b				
$\rho(r_c)$		0.283	0.255	0.223
$\nabla^2\rho(r_c)$		3.472	2.594	1.812
ϵ		0.069	0.077	0.083
r_t				
$\rho(r_c)$	0.520	0.337	0.302	0.262
$\nabla^2\rho(r_c)$	8.736	4.230	3.090	2.122
ϵ	0.000	0.000	0.000	0.000
Li−X				
$\rho(r_c)$		0.067	0.062	0.056
$\nabla^2\rho(r_c)$		0.694	0.521	0.395
ϵ		0.069	0.077	0.083

[a] Calculated at the MP2/B′ level; for details of basis set see text. Charge density at the critical point $\rho(r_c)$ (e $Å^{-3}$); Laplacian at the critical point $\nabla^2\rho(r_c)$ (e $Å^{-5}$). The abbreviations b and t mean bridged and terminal, respectively (cf. Figure 1).

Figure 4 illustrates significant differences between the vibrational spectra of structures 2 and 3. Structure 3 has fewer vibrational bands compared to structure 2, due to degeneracies in the C_{3v} point group. Generally, three of the eight fundamentals of structure 3 and four to six of the total 12 fundamentals of structure 2 have considerable IR intensity. Very strong bands belong to some Ln−X stretching modes of structure 3 positioned in the middle of the IR spectra. However, the most characteristic difference between the spectra of the two structures appears in the region of the Li−X stretching vibrations. This highest fundamental frequency of structures 2 is positioned ca. 100 cm^{-1} higher than the respective Li−X fundamental of structures 3. The frequency values of these Li−X stretching vibrations correlate well with the Li−X bond distances of the two structures (vide supra). The characteristics of the IR spectra of both possible structures outlined above should, in principle, provide a possibility to distinguish unambiguously between the two structures.

Considering the Raman spectra, we should note the less reliability of computed Raman activities than found for the IR intensities, which makes a prediction based on computations more ambiguous. Moreover, the computed Raman spectra of the two structures look more similar than found in the case of

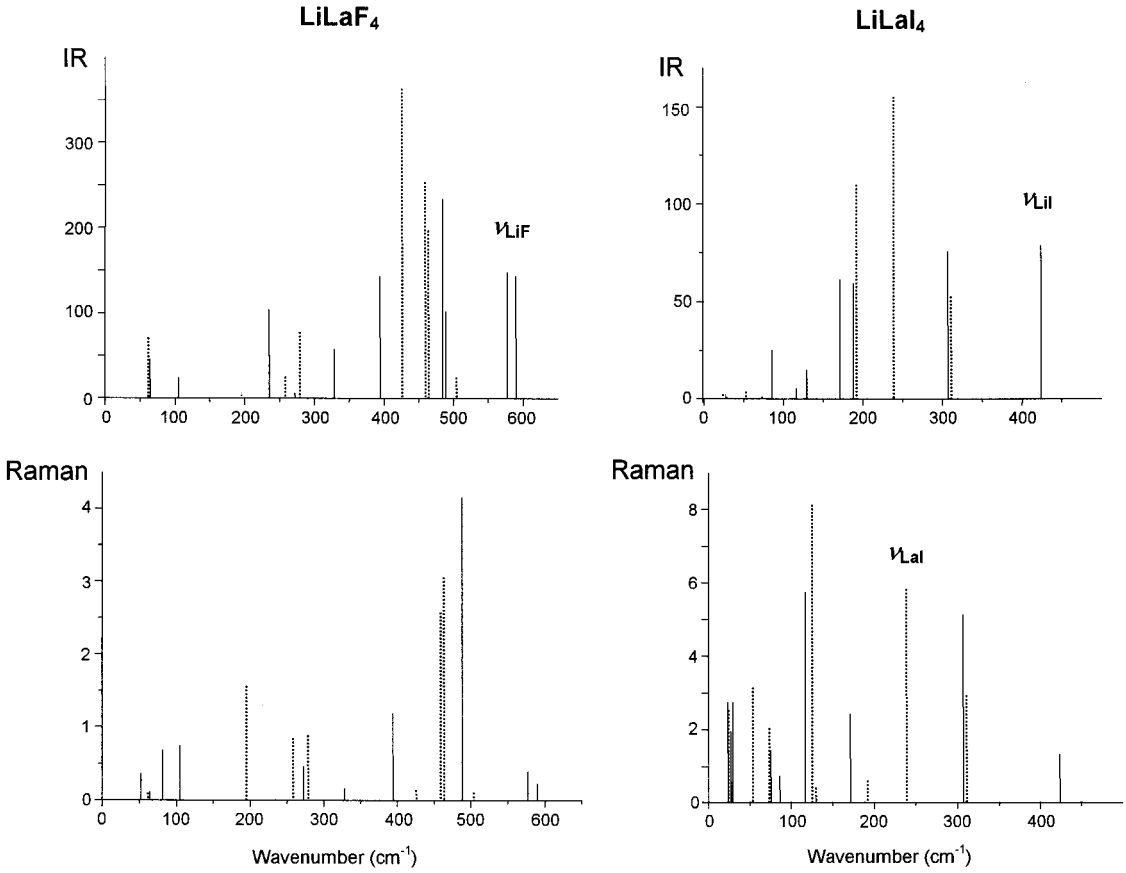

Figure 4. Calculated vibrational spectra of the bi- (solid line) and tridentate (dotted line) structures of $LiLaF_4$ and $LiLaI_4$. Units of the calculated IR and Raman intensities are km/mol and Å^4/amu, respectively.

IR. Due to the comparable Raman activity of most of the fundamentals, the spectra are also more crowded. Most characteristic is again the highest frequency Li−X stretching band of structures 2, in which range structures 3 have no fundamentals. However, the Raman activity of this band might be too weak (close to the magnitude of overtones and combination bands) for an unambiguous identification of structure 2 in a complex vapor. An additional feature with indicator character may be the asymmetric Ln−X stretching band of structures 3 of bromides and iodides around 250 cm^{-1}, appearing in a relatively uncrowded range with considerable calculated activity. Altogether, an unambiguous assignment of the structure of the $LiLnX_4$ complexes on the basis of the Raman spectrum is less probable.

Conclusions

The present calculations indicate the superiority of MP2 theory over the HF and B3-LYP methods regarding the energetics of $LiLnX_4$ coordination complexes and point to the importance of *f* polarization functions in the basis sets of the alkali metal and the halogens for a proper description of the Li···X interaction.

Our study confirmed the significance of the mono- (C_{3v}), bi- (C_{2v}), and tridentate (C_{3v}) structures for $LiLnX_4$ complexes. At the MP2/B level the bidentate structure is definitely the global minimum in the fluoride complexes, but with heavier halogens the bi- and tridentate forms get closer in energy and in the iodide complexes the relative order of stability is reversed. The monodentate structure was found to be a saddle point except for the fluorides where it is a high-lying local minimum. The energy difference between the different structures as well as the dissociation energy decreases in the row F to I. The contribution of the entropy at the experimentally meaningful high temperatures may support the predominance of structure 2 in a thermodynamical equilibrium, even in the case of the iodide systems.

In accordance with the observed trends in the relative energies, the geometrical parameters indicate a more favored coordination of Li in structure 3 with increasing halogen size. The NBO atomic charges and the results of the topological analysis of the charge distribution are in agreement with strong ionic interactions in the title complexes. Minor covalent contributions appear in the complexes with heavier halogens as well as with increasing coordination of Li. Variation of the geometrical and bonding characteristics between the lanthanum and dysprosium complexes reflect the effect of "lanthanide contraction".

The vibrational (IR and Raman) spectra of the chemically relevant structures 2 and 3 have characteristic features, based on which the complexes can be identified in the vapor phase. In principle, the two structures can be distinguished unambiguously by their infrared spectra.

Acknowledgment. This research has been supported by STW (Project No. ACH3757). A.K. thanks the Bolyai Foundation for a fellowship and the Hungarian Scientific Research Foundation (OTKA, No. F 022170) and the Ministry of Education of Hungary (FKFP 0364/1999) for financial support.

Supporting Information Available: Vibrational frequencies of structures 1−3 calculated at the MP2/A level as well as IR and Raman activities. This material is available free of charge via the Internet at http://pubs.acs.org.

IC000581T